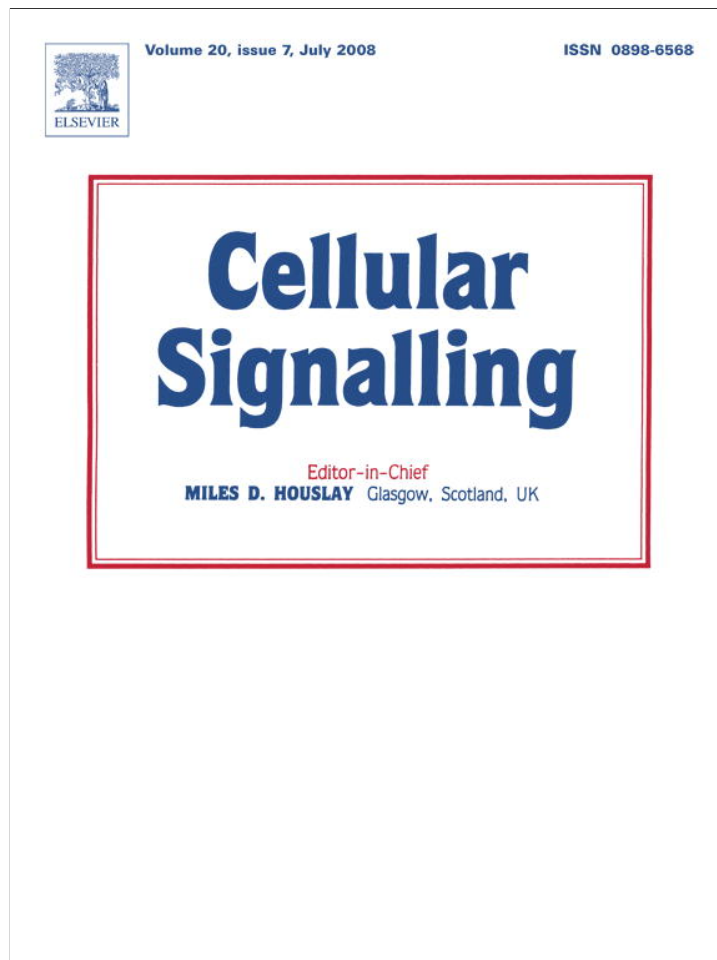


Provided for non-commercial research and education use.
Not for reproduction, distribution or commercial use.



This article appeared in a journal published by Elsevier. The attached copy is furnished to the author for internal non-commercial research and education use, including for instruction at the authors institution and sharing with colleagues.

Other uses, including reproduction and distribution, or selling or licensing copies, or posting to personal, institutional or third party websites are prohibited.

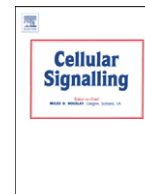
In most cases authors are permitted to post their version of the article (e.g. in Word or Tex form) to their personal website or institutional repository. Authors requiring further information regarding Elsevier's archiving and manuscript policies are encouraged to visit:

<http://www.elsevier.com/copyright>



Contents lists available at ScienceDirect

Cellular Signalling

journal homepage: www.elsevier.com/locate/cellsig

Oxidative stress and calpain inhibition induce alpha B-crystallin phosphorylation via p38-MAPK and calcium signalling pathways in H9c2 cells

Ioanna-Katerina S. Aggeli, Isidoros Beis, Catherine Gaitanaki *

Department of Animal and Human Physiology, School of Biology, Faculty of Sciences, University of Athens, Panepistimioupolis Ilissia, 157 84 Athens, Greece

ARTICLE INFO

Article history:

Received 7 January 2008

Received in revised form 25 February 2008

Accepted 25 February 2008

Available online 4 March 2008

Keywords:

Alpha B-crystallin

Oxidative stress

Calpain inhibition

Cardiac myocytes

Signalling

p38-MAPK

Calcium

Apoptosis

ABSTRACT

We investigated the response of α B-crystallin to oxidative stress and calpain inhibition in an attempt to elucidate the signalling pathways mediating its phosphorylation. Given the high expression levels of α B-crystallin in cardiac muscle one can evaluate the significance of its participation in preservation of homeostasis under adverse conditions. H9c2 cardiac myoblasts were used as our experimental model since their response reflects the signal transduction pathways activated by stress conditions in the myocardium. Thus, in H9c2 cells treated with H_2O_2 the mechanism regulating α B-crystallin phosphorylation was found to involve p38-MAPK/MSK1 as well as intracellular free calcium levels. Our immunocytochemical experiments demonstrated phosphorylated α B-crystallin to be co-localized with tubulin, potentially preserving cytoskeletal architecture under these interventions. In H9c2 cells treated with calpain inhibitors (ALLN, ALLM) α B-crystallin exhibited a p38-MAPK- and $[Ca^{2+}]_i$ -dependent phosphorylation pattern since the latter was ablated in the presence of the selective p38-MAPK inhibitor SB203580 and calcium chelator BAPTA-AM. Calpain activity repression ultimately led to apoptosis confirmed by PARP fragmentation and chromatin condensation. However, the apoptotic pathway activated by ALLM and ALLN differed, underlying the diverse transduction mechanisms stimulated. In addition to this, an anti-apoptotic role for phospho- α B-crystallin was verified by confirmation of its interaction with pro-caspase 3, hindering its cleavage and subsequent activation. Collectively, our findings underline α B-crystallin crucial role as a participant of cardiac cells early response to stressful stimuli compromising their survival.

© 2008 Elsevier Inc. All rights reserved.

1. Introduction

Throughout their life span cells are exposed to multiple adverse conditions; response to these stress factors ultimately determines the fate of tissues, organs and consequently of whole organisms [1]. Heat shock proteins (Hsps) constitute a superfamily whose members function as chaperones contributing to cell survival. Small heat shock proteins (sHsps) are less than 43 kDa in mass and are characterized by a conserved α -crystallin C-terminal domain [2]. An intriguing property of some sHsps, including Hsp27 and α B-crystallin (α Bcr), is their rapid phosphorylation in response to variable stimuli, modulating their activity [3] by modifying the globular oligomeric structures they form [4]. This phosphorylation has been shown to mediate protection against various stressful conditions stabilizing other proteins i.e. phosphorylated α Bcr has been reported to interact with microtubules as well as intermediate filaments contributing to

preservation of cytoskeletal integrity [5]. A plethora of studies have confirmed MAPKs prominent role in the signal transduction pathways involved in α Bcr phosphorylation [6] but the physiological role that the latter plays in the context of cellular defense under stressful stimuli remains elusive.

MAPKs represent a highly conserved superfamily of serine/threonine protein kinases. There are three best-characterized MAPK subfamilies: extracellular signal-regulated kinases (ERKs), cJun-N-terminal kinases (JNKs) and p38-MAPK [7]. Activated MAPKs are localized in both the cytoplasm and nucleus, where they interact with their substrates including: other protein kinases (i.e. MSK1), cytoskeletal proteins [8], transcription factors [7,8] and α Bcr [9].

The ability of the cardiac muscle to mount an efficient defense against stressful conditions that can potentially harm it is of paramount importance for survival. Heart function can be compromised by ischemic episodes, toxins, reactive oxygen species (ROS), protein impairments and defective clearance of damaged proteins [10]. Thus, protein quality control exerted by molecular chaperones and the proteasome, act in a cardioprotective manner preventing activation of pathways prone to lead to apoptosis. Apoptosis may be triggered by several physiological or pathological stimuli and is executed by caspases that can be activated by signal transduction pathways associated with stimulation of death receptors (extrinsic

Abbreviations: MAPK, mitogen-activated protein kinase; MSK1, mitogen and stress-activated kinase; α Bcr, alpha B-crystallin; PARP, poly-(ADP-ribose) polymerase; ALLN, N-Acetyl-Leu-Leu-Norleucinal; ALLM, N-Acetyl-Leu-Leu-Methioninal; FITC, fluorescein-isothiocyanate isomer 1; TRITC, tetramethylrhodamine isomer R.

* Corresponding author. Tel.: +30 210 7274136; fax: +30 210 7274635.

E-mail address: cgaitan@biol.uoa.gr (C. Gaitanaki).

pathway) or mitochondrial stress (intrinsic pathway) leading to the release of cytochrome *c* and triggering of downstream effector caspases [11].

Several scientific groups have reported protein proteolysis to be of significant importance in the apoptotic process, underlying the role of proteases in apoptosis [12]. One family of proteases shown to be involved in the latter are the calpains with their two ubiquitously expressed isoforms (calpain I and II) best characterized and defined for their calcium-dependent activation [13].

α Bcrystallin is a major protein in ocular lens contributing to preservation of its transparency and refractive properties [14], counteracting lens opacification resulting from thermal impacts, oxidative stress and calcium accumulation, also leading to repression of apoptosis [15]. What is more, it has been found to act as an antioxidant and free radical scavenger decreasing thiol groups oxidation [16]. Quite surprisingly, α Bcrystallin expression levels are exquisitely high in cardiac muscle where it constitutes more than 3% of total protein content [17]. Therefore, elucidating α Bcrystallin physiological role in cardiac myocytes exposed to oxidative insults is extremely interesting. Moreover, taking into account the reported proteolysis of α -crystallins by calpain *in vitro* [18] and in selenite cataract [19], along with the enhanced intracellular calcium concentration confirmed to modulate apoptosis mediating-protease activity [20], examining α Bcrystallin response to calpain inhibition also appeared intriguing.

Thus, in the present study we investigated α Bcrystallin phosphorylation pattern induced by oxidative stress (simulated by H₂O₂) and calpain inhibition (using two known calpain inhibitors: ALLM and ALLN) in H9c2 cardiomyoblasts, a clonal cell line derived from embryonic heart ventricle [21], which retains properties of signalling pathways of adult cardiomyocytes. Several research groups have proven that any finding in H9c2 cells reflects the transduction pathways activated in the complex and of diverse cell populations comprised myocardium and this fact justifies the great number of reports using H9c2 myoblasts as an experimental model in order to investigate stress effects on the cardiomyocyte [22]. In the case of H₂O₂-treated H9c2 cardiac myoblasts, p38-MAPK/MSK1 pathway was shown to mediate the observed effect, leading to interaction of phosphorylated α Bcrystallin with tubulin. Treatment of H9c2 cells with calpain inhibitors initially stimulated p38-MAPK-mediated α Bcrystallin phosphorylation. The intensity and duration of these particular stimuli were such that eventually led to apoptosis via diverse signalling pathways determined for the first time in cardiac myoblasts. Overall our results show α Bcrystallin to be phosphorylated possibly participating in a first line of defense against stimuli that disturb the cellular redox balance or cellular protein control equilibrium, exhibiting ultimately detrimental effects for cardiac myocytes.

2. Materials and methods

2.1. Materials

Hydrogen peroxide was purchased from Merck (Darmstadt, Germany). *N*-Acetyl-Leu-Leu-Norleucinal (ALLN), *N*-Acetyl-Leu-Leu-Methioninal (ALLM), DMSO, leupeptin, *trans*-epoxy-succinyl-L-leucylamido-(4-guanidino) butane (E-64), dithiothreitol (DTT), phenylmethylsulphonyl fluoride (PMSF), 4 β -phorbol 12-myristate 13-acetate (PMA), ethylenediamine-N,N'-bis-(2-aminophenoxy) ethane-N,N,N',N'-tetraacetic acid tetrakis (acetoxymethyl ester) (BAPTA-AM), Hoechst 33258-bisbenzamide (Hoechst) and protein A-Sepharose were obtained from Sigma-Aldrich (St Louis, Missouri, USA). SP600125 and PD98059 were purchased from Calbiochem-Novabiochem (La Jolla, CA, USA). SB203580, PKI-tide and H89 were from Alexis Biochemicals (Lausen, Switzerland). Nitrocellulose (0.45 μ m) was obtained from Schleicher & Schuell (Keene NH, USA). Prestained molecular mass markers were from New England Biolabs (Beverly, MA, USA). Secondary antibodies were from DakoCytomation (Glostrup, Denmark). Super RX film was purchased from Fuji photo film GmbH (Dusseldorf, Germany). General laboratory reagents were purchased from Sigma-Aldrich or Merck.

2.2. Cell cultures and reagents

H9c2 cells (passage 18–25; American Type Culture Collection, Rockville, MD, USA) were cultured in DMEM (PAA Laboratories GmbH, Pasching, Austria) supplemented with 10% (v/v) heat inactivated fetal bovine serum (PAA Laboratories GmbH) and antibiotics

(plating medium), under an atmosphere of 95% air/5% CO₂ at 37 °C. Experiments were carried out using mononucleated myoblasts after serum had been withdrawn for 24 h. Hydrogen peroxide, ALLM and ALLN were added to the medium for the times and at the doses indicated. ALLM and ALLN as well as the pharmacological inhibitors used were dissolved in DMSO. Inhibitors were added to the medium 30 min prior to treatment. Control experiments with DMSO alone were also performed for the same duration.

2.3. Protein extraction

Cells were extracted in buffer G [20 mM Tris-HCl pH 7.5, 20 mM β -glycerophosphate, 2 mM EDTA, 10 mM benzimidazole, 20 mM NaF, 0.2 mM Na₂VO₄, 200 μ M leupeptin, 10 μ M E-64, 5 mM DTT, 300 μ M PMSF and 0.5% (v/v) Triton X-100]. Sample preparation was subsequently performed as described in our previous work [23].

2.4. Preparation of mitochondrial extracts

Levels of cytochrome *c* were analyzed in mitochondrial and cytosolic cell fractions. Mitochondria were isolated according to the method described by Gottlieb and Granville, 2002 [24] with slight modifications. In particular, cells were extracted in buffer M (250 mM sucrose, 20 mM K⁺ Hepes, 10 mM KCl, 1.5 mM MgCl₂, 0.1 mM EDTA, 1 mM EGTA, 1 mM DTT and 200 μ M PMSF) and incubated at 4 °C for 20 min. Extracts were centrifuged twice (5700 rpm, 5 min, 4 °C) and the resulting supernatants were centrifuged at 9700 rpm for 15 min (4 °C). Pellets were resuspended in buffer M containing 0.1% (v/v) Triton X-100, centrifuged (10,000 rpm, 5 min, 4 °C) and supernatants were boiled with 0.33 vol. of SDS-PAGE sample buffer. Protein concentrations were determined using the BioRad Bradford assay reagent (Bio-Rad, Hercules, California, USA).

2.5. Immunoblotting

Proteins were separated by SDS-PAGE on 10% (w/v) polyacrylamide gels and transferred electrophoretically onto nitrocellulose membranes. Nonspecific binding sites were blocked and subsequently, membranes were incubated overnight with the appropriate primary antibody (1:1000) at 4 °C. Antibodies against caspase 3, cytochrome *c*, poly (ADP-ribose) polymerase (PARP), phospho-ERKs and phospho-p38-MAPK, were from Cell Signalling Technology (Beverly, MA, USA), anti-actin was from Sigma-Aldrich (St Louis, Missouri, USA). Dr W. Boelens kindly provided us with the antibody detecting total levels of α B-crystallin while antibodies against phosphorylated- α B-crystallin (Ser 19, 45, 59) were a kind gift from Dr H. Ito. Next, blots were manipulated as described in our previous work [48] and bands were detected using enhanced chemiluminescence (ECL) (Amersham Biosciences, Uppsala, Sweden) and quantified by scanning densitometry (Gel Analyzer v. 1.0).

2.6. Immunofluorescence staining

Cells were grown on appropriate chamber slides in plating medium and were treated after serum had been withdrawn for 24 h. Subsequently, cells were fixed with 4% (v/v) formaldehyde in phosphate buffer saline (PBS) pH 7.4 for 15 min at R_T, washed in PBS (\times 3) and incubated (5 min, R_T) with 1% (w/v) BSA in PBS containing 0.3% (v/v) Triton X-100. Incubation with the primary antibody against phospho- α B-crystallin (Ser59) (1:100, 1 h, 37 °C) was followed by 1 h incubation at 37 °C with either a FITC-conjugated anti-rabbit secondary antibody (green fluorescence) or alternatively with a TRITC-conjugated anti-rabbit secondary antibody (red fluorescence). Secondary antibodies were provided by DAKOCytomation (Glostrup, Denmark). When the monoclonal anti-tubulin antibody kindly provided by Dr. Apostolakis (University of Athens, Greece) was used (1:300, 1 h, 37 °C) cells were washed and subsequently incubated with a FITC-conjugated anti-mouse secondary antibody (DAKOCytomation). After washing, cell nuclei were stained using Hoechst 33258 (0.001 μ g/ml). Following mounting, chamber slides were visualized under a Zeiss-Axioplan fluorescence microscope.

2.7. Immunoprecipitation

30 μ l of protein A-Sepharose [50% slurry in RBD buffer: 20 mM Tris-HCl pH 7.5, 1 mM EDTA, 1% (v/v) Triton X-100, 10% (v/v) glycerol, 100 mM KCl, 5 mM NaF, 0.2 mM Na₂VO₄, 5 mM MgCl₂, 0.05% (v/v) 2-mercaptoethanol] were incubated with 2 μ l of caspase 3 antibody on a rotating wheel (4 °C, O/N). After a brief spin (10,000 rpm, 1 min, 4 °C) the formed complexes were washed in RBD buffer (\times 3). Untreated (control) or ALLM-treated cells (2 h and 3 h) were scraped into RBD buffer containing 200 μ M leupeptin, 10 μ M E-64, 5 mM DTT and 300 μ M PMSF. Samples were extracted on ice (10 min) and centrifuged (10,000 rpm, 5 min, 4 °C). An aliquot of the supernatants was boiled with 0.33 vol. of SB4X, while the rest was incubated with the protein A-Sepharose/antibody complexes (4 h, 4 °C). After centrifugation (10,000 rpm, 1 min, 4 °C) the supernatants (S/N) were boiled with 0.33 vol. of SB4X. Pellets were washed (\times 3) with RBD buffer and finally resuspended (immunoprecipitate-IP) and boiled in 40 μ l of (SB2X). The reverse protocol was also performed using 2 μ l of phospho- α B-crystallin (Ser59) antibody.

2.8. Statistical evaluations

All data are presented as means \pm S.E.M. Comparisons between control and treatment were performed using Student's paired *t*-test. A value of at least *p* < 0.05 was considered to be statistically significant.

3. Results

3.1. H₂O₂ induces alpha B-crystallin phosphorylation in H9c2 cells. Involvement of p38-MAPK / MSK1 and calcium signalling pathways

Alpha B-crystallin (α Bcr) is constitutively expressed in high concentrations (2–3% of total protein content) in the myocardium of rats. Given the protective role this sHsp plays against several chemical and physical stress challenges encountered by the heart [25,26], we first investigated its expression profile in H9c2 cardiac myoblasts exposed to oxidative stress in the form of 200 μ M H₂O₂, a concentration used routinely in cardiomyocyte experimental settings [27]. Under these oxidative conditions no fluctuation was detected in α Bcr mRNA levels (data not shown) neither in total α Bcr protein levels (Fig. 1A bottom panel) examined by semi-quantitative RT-PCR and

immunoblotting analysis, respectively. Accumulating evidence suggests that post-translational modifications regulate α Bcr function [28] we therefore examined its time-dependent phosphorylation pattern in cells exposed to H₂O₂. This sHsp is known to be phosphorylated on three serine residues: 19, 45, and 59 [28] but we focused on Ser59 since no significant signal was detected when immunoblotting with antibodies recognizing α Bcr phosphorylated at Ser19 nor at Ser45 (data not shown). In particular, a rapid onset of α Bcr phosphorylation was observed at 15 min (2.1 \pm 0.04 fold relative to control) with maximal values being attained at 2 h (5.1 \pm 0.07 fold relative to control), decreasing thereafter (Fig. 1A upper panel and E). So as to decipher the signalling pathways involved in this response several pharmacological inhibitors were used: SB203580 (10 μ M): a p38-MAPK inhibitor, PD98059 (25 μ M) that blocks the ERK1/2 pathway, SP600125 (10 μ M): a JNKs inhibitor, PKI (10 μ M): inhibiting PKA, PMA

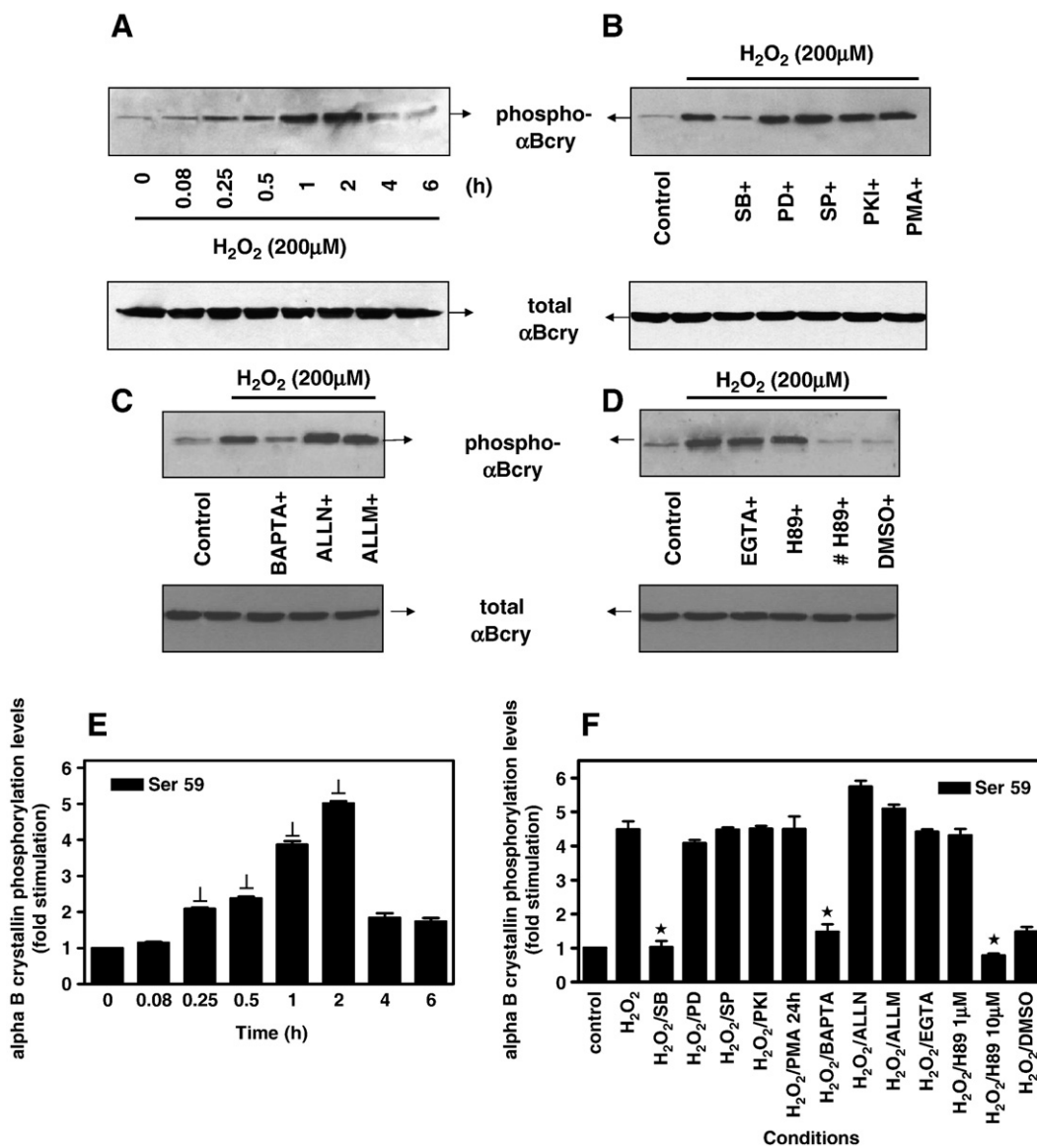


Fig. 1. Profile of H₂O₂-induced alpha B-crystallin (α Bcr) phosphorylation at Ser59 in H9c2 cardiomyoblasts; a p38-MAPK, MSK1 and intracellular calcium-dependent response. (A) H9c2 cells were exposed to 200 μ M H₂O₂ for the times indicated. (B) H9c2 cells were left untreated (control) or pre-incubated with 10 μ M SB203580, 25 μ M PD98059, 10 μ M SP600125, 10 μ M PKI, 1 μ M PMA, 10 μ M BAPTA-AM, 20 μ M ALLN, 100 μ M ALLM, 10 mM EGTA, H89 at either 1 or 10 μ M (#), DMSO and were then exposed to 200 μ M H₂O₂ for 2 h in the absence or presence of the inhibitors. Cell extracts (20 μ g) were subjected to SDS-PAGE and immunoblotted with an antibody for phosphorylated α Bcr (Ser59) (A and B upper panels, C and D). To verify equal loading, the membranes were then stripped and re-incubated with an antibody against total α Bcr levels (A and B bottom panels). Bands were quantified by laser scanning densitometry (E and F). Blots and results shown are representative of at least three independent experiments. Results are means \pm SEM for at least three independent experiments. $p < 0.001$, compared to control values; * $p < 0.001$ compared to identically treated cells in the absence of inhibitors.

(1 μM for 24 h): used to inhibit PKC, BAPTA-AM (10 μM): a cell-permeable chelator of intracellular calcium stores, ALLN (20 μM) and ALLM (100 μM): both widely used calpain inhibitors, EGTA (10 mM): an agent chelating extracellular calcium and H89 at 1 μM blocking PKA and at 10 μM shown to inhibit MSK1. Cells were left untreated (control) or were incubated with a) either DMSO (Fig. 1D last lane), b) the inhibitors alone (data not shown) or c) with the inhibitors followed by exposure to 200 μM H_2O_2 for 2 h. DMSO as well as most of the inhibitors alone (SB203580, PD98059, SP600125, PKI, PMA, BAPTA-AM, EGTA, H89) had no effect on αBcr_y phosphorylation levels. As shown in Fig. 1B (upper panel), C, D and F, pretreatment of H9c2 cells with SB203580, BAPTA-AM and H89 at 10 μM , markedly reduced H_2O_2 -stimulated αBcr_y phosphorylation. On the other hand, the latter was enhanced in the presence of ALLN and ALLM, while PD98059, SP600125, PKI, PMA, EGTA and H89 at 1 μM failed to change the observed response. These results indicate that p38-MAPK, MSK1 and intracellular calcium levels participate in the mechanism regulating H_2O_2 -induced αBcr_y phosphorylation in H9c2 cells. In contrast, ERKs, JNKs, PKA, PKC as well as extracellular calcium levels do not seem to contribute to the observed response. Total levels of αBcr_y did not change during these interventions, with representative blots presented in Fig. 1A and B (bottom panels).

3.2. Distribution pattern of αBcr_y immunoreactivity in H_2O_2 -treated H9c2 cells

Subsequently, we investigated αBcr_y distribution pattern so as to help us identify and elucidate the possible biological function of phosphorylated αBcr_y following oxidative stress, a stimulus that has been shown to have detrimental effects on cardiac myocytes-causing apoptosis [29]. We thus examined αBcr_y localization using the same phospho-specific anti- αBcr_y (Ser59) antibody. The immunofluorescence signal was almost undetectable in untreated cells (control) (Fig. 2A and C) with only nuclei being discernible with Hoechst 33258 staining (Fig. 2B). Conversely, treatment of H9c2 cells with 200 μM H_2O_2 for 2 h revealed a perinuclear (Fig. 2D) as well as punctuate cytoplasmic distribution (Fig. 2E) of phosphorylated αBcr_y .

Given the association of αBcr_y with several cytoskeletal elements under stress conditions [30] we decided to assess any possible co-localization of phosphorylated αBcr_y under the above experimental conditions. Indeed, co-localization areas of phospho- αBcr_y (Fig. 3D) with tubulin (Fig. 3B) were found in the cytoplasm of H_2O_2 -treated H9c2 cells (Fig. 3E, merged). Nuclei were once more stained with Hoechst (Fig. 3C) while tubulin immunoreactivity in untreated (control) cells is presented in Fig. 3A. No immunoreactivity was observed in cells incubated solely with the respective secondary antibodies (data not shown).

3.3. Calpain inhibitors ALLN and ALLM induce αBcr_y phosphorylation in H9c2 cells

In light of the apparent additive and synergistic effect of both ALLN and ALLM on H_2O_2 -induced αBcr_y phosphorylation (Fig. 1C: 4th and 5th lines) we made an effort to delineate these calpain inhibitors' effect on the latter, given the controversy that exists regarding the pro- or anti-apoptotic effect they have depending on cell type and the apoptotic stimulus involved [31 vs. 32]. Therefore, after evaluating the minimal concentration of ALLN (20 μM) and ALLM (100 μM) that reproducibly stimulates αBcr_y phosphorylation (data not shown), the time-dependent pattern of the latter was investigated. As shown in Fig. 4A (upper panel) and C, ALLN markedly stimulated αBcr_y phosphorylation levels with maximal values attained at 2 h (5.2 ± 0.2 fold relative to control). A similar time profile was induced by ALLM with maximal phosphorylation observed at 2 h but the magnitude of the response was less (3.1 ± 0.17 fold relative to control) (Fig. 4B upper panel and D). Total levels of αBcr_y remained unchanged during these interventions (Fig. 4A and B, bottom panels). In order to elucidate the signal transduction cascades activated under the conditions examined the effect of pretreatment with several inhibitors was studied. SB203580 as well as BAPTA-AM ablated ALLN- (Fig. 5A and C) and ALLM- (Fig. 5B and D) induced αBcr_y phosphorylation, implicating p38-MAPK and intracellular calcium signalling in the mechanism regulating this response. On the other hand, neither ERKs, JNKs, PKA nor MSK1 were found to participate in stimulation of the observed phosphorylation.

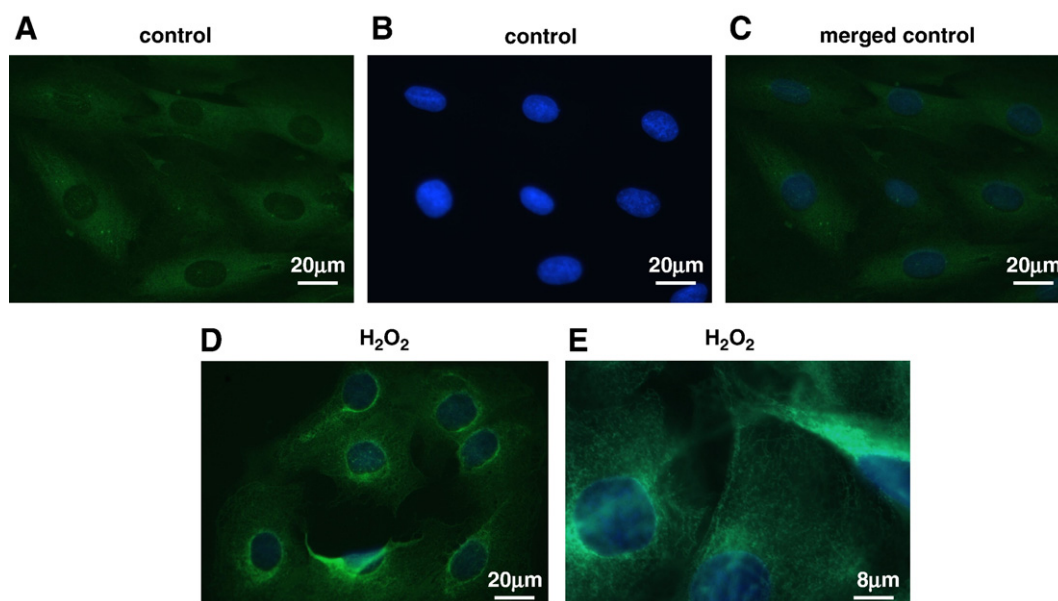


Fig. 2. Localization profile of phosphorylated αBcr_y in H9c2 cardiomyoblasts left untreated (control) or exposed to 200 μM H_2O_2 for 2 h. Cells were subjected to immunocytochemical analysis with an antibody directed against phosphorylated αBcr_y (Ser59) (green fluorescence). To reveal nuclear morphology nuclei were stained with Hoechst 33258. Representative images are shown, indicative of at least three independent experiments. C: A+B, merged. (For interpretation of the references to colour in this figure legend, the reader is referred to the web version of this article.)

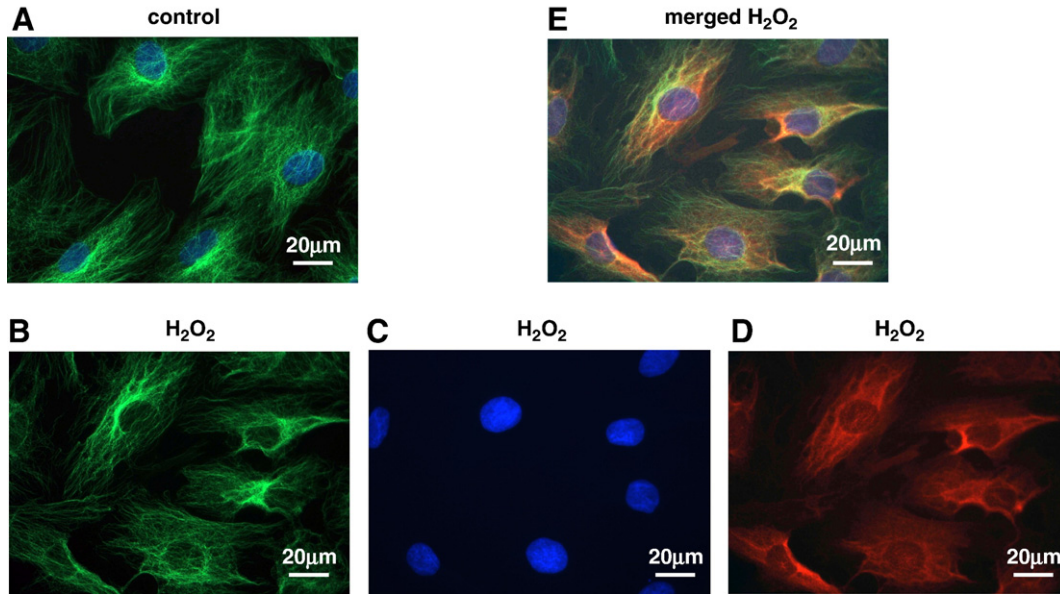


Fig. 3. Co-localization areas of phosphorylated α Bcryst and tubulin in H9c2 cardiomyoblasts left untreated (control) or exposed to 200 μ M H_2O_2 for 2 h. Cells were subjected to double immunofluorescence staining with a monoclonal antibody directed against tubulin (green) and a polyclonal antibody against phosphorylated α Bcryst (Ser59) (red fluorescence). To reveal nuclear morphology nuclei were stained with Hoechst 33258. Representative images are shown, indicative of at least three independent experiments. E: B+C+D, merged.

3.4. ALLN and ALLM induce p38-MAPK and ERKs phosphorylation in H9c2 cells

Given that MAPKs consist fundamental intracellular signalling molecules and with the revealed implication of p38-MAPK in ALLN- and ALLM-induced α Bcryst phosphorylation, the activation profile of all three major MAPK subfamilies was investigated. Immunoblotting for the phosphorylated form of p38-MAPK revealed the kinase activation which became maximal after 4 h treatment with ALLN (5.2 ± 0.25 fold relative

to control) (Fig. 6A upper panel and C) as well as ALLM (3.4 ± 0.37 fold relative to control) (Fig. 6B upper panel and D). On the contrary, JNKs were not found to participate in the mechanism transducing the particular signal (data not shown). Furthermore, although use of PD98059 (an ERKs activity inhibitor) did not affect α Bcryst phosphorylation at Ser59 by ALLN nor by ALLM (Fig. 5A and B, 3rd lines), ERKs were found to be activated by both agents exhibiting a differential pattern. In particular, as shown in Fig. 6A (middle panel) and E, ALLN caused a significant upregulation of ERKs phosphorylation maximized at 2 h

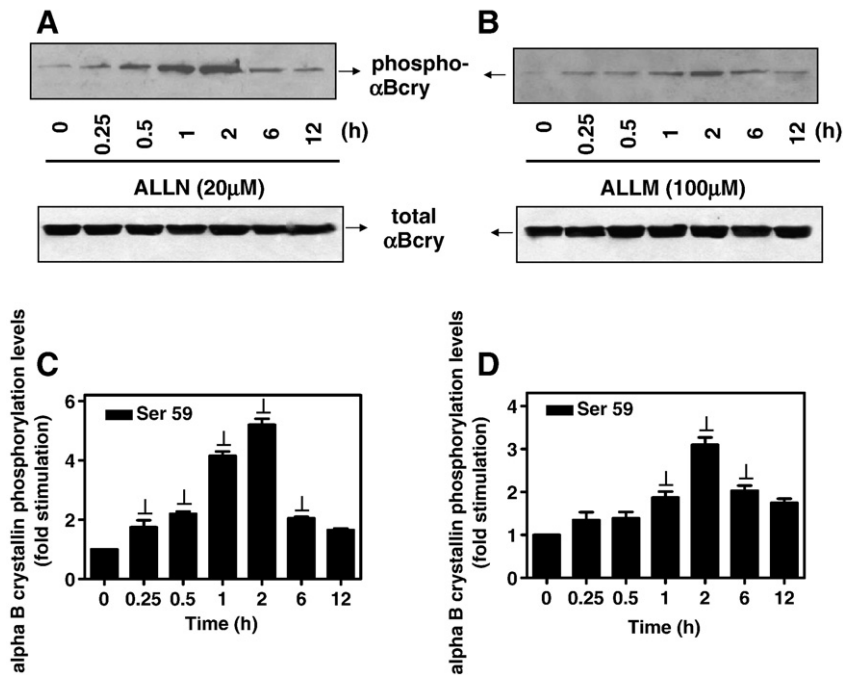


Fig. 4. Time course of ALLN- (20 μ M) (A) and ALLM- (100 μ M) (B)-induced α Bcryst phosphorylation in H9c2 cardiomyoblasts. H9c2 cells were exposed to 200 μ M H_2O_2 for the times indicated. Cell extracts (20 μ g) were subjected to SDS-PAGE and immunoblotted with an antibody for phosphorylated α Bcryst (Ser59) (A and B upper panels). To verify equal loading, the membranes were then stripped and re-incubated with an antibody recognizing total α Bcryst levels (A and B bottom panels). Bands were quantified by laser scanning densitometry (C and D). Blots and results shown are representative of at least three independent experiments. Results are means \pm SEM for at least three independent experiments. $p < 0.001$, compared to control values.

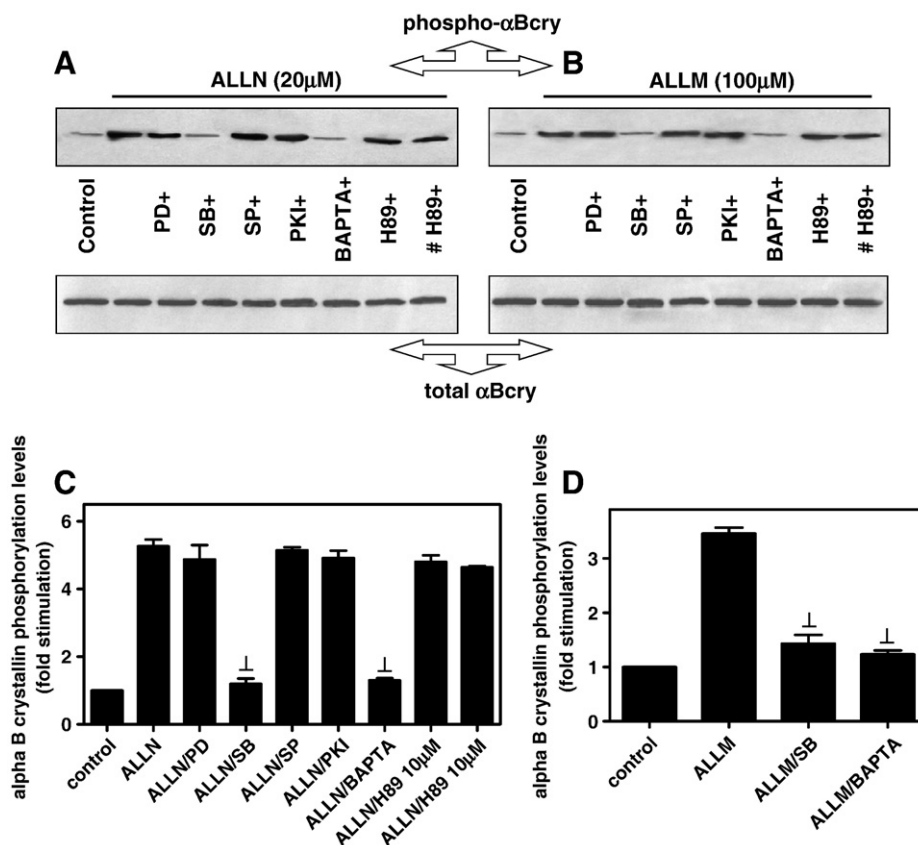


Fig. 5. Effect of pharmacological inhibitors on ALLN- (20 μ M) (A) and ALLM- (100 μ M) (B)-induced α Bcrystallin phosphorylation in H9c2 cardiomyoblasts. H9c2 cells were left untreated (control) or pre-incubated with the inhibitors indicated and were then exposed to 20 μ M ALLN or 100 μ M ALLM for 2 h in the absence or presence of the inhibitors. Cell extracts (20 μ g) were subjected to SDS-PAGE and immunoblotted with an antibody for phosphorylated α Bcrystallin (Ser59) (A and B upper panels). To verify equal loading, the membranes were then stripped and re-incubated with an antibody against total α Bcrystallin levels (A and B bottom panels). Bands were quantified by laser scanning densitometry (C and D). Blots and results shown are representative of at least three independent experiments. Results are means \pm SEM for at least three independent experiments. $p < 0.001$, compared to identically treated cells in the absence of inhibitors.

(6.25 ± 0.25 fold relative to control) while ALLM effect was more rapid, with ERKs attaining maximal phosphorylation at 30 min (6.75 ± 0.35 fold relative to control) (Fig. 6B middle panel and F). Equal protein loading was verified by reprobing the membranes with an anti-actin antibody (Fig. 6A and B, bottom panels). Given the observed involvement of both p38-MAPK and intracellular calcium in the mechanism mediating α Bcrystallin phosphorylation under the conditions investigated we decided to make an effort so as to clarify whether these signals are sequential or parallel. To this end, p38-MAPK phosphorylation was examined by immunoblot analysis in samples from cells treated with ALLM, ALLN as well as H_2O_2 in the presence or absence of the calcium chelator BAPTA-AM. As shown in Fig. 7A upper panel and B, BAPTA-AM induces p38-MAPK phosphorylation (5.85 ± 0.55 fold relative to control [1.5 h] or 4.57 ± 0.42 fold relative to control [45 min]). After subtracting this effect, BAPTA-AM is revealed to inhibit p38-MAPK phosphorylation by the agents examined. Reprobing with an antibody against total α Bcrystallin we verified equal protein loading (Fig. 7A bottom panel). This finding is indicative of a pathway where intracellular calcium appears to “operate” upstream of p38-MAPK which subsequently transduces the stimulus involved to α Bcrystallin. Further studies are indispensable however in order to fully elucidate the sequence of events regulating these responses.

3.5. ALLN and ALLM cause apoptosis in H9c2 cells

The conflicting reports on ALLN and ALLM protective [33] or detrimental [34] role in various experimental settings, prompted us to monitor the biological impact that ALLN and ALLM actually have on H9c2 cardiac myoblasts. To this end, the proteolytic processing of

PARP was examined, a marker routinely used to monitor apoptotic cell death [35]. Thus, 6 h and 12 h treatment with ALLN was found to considerably increase the intensity of the caspase 3 generated 89 kDa PARP fragment [36] with an even more profound band intensity observed after treatment with ALLM for similar time periods (Fig. 8). When samples from cells treated with either ALLM or ALLN for 2 h or 4 h were processed, no PARP fragmentation was detected (data not shown). The nature of the upper band of approximately 95 kDa molecular mass, whose intensity appears to change in parallel with that of the 89 kDa fragment is under investigation and may represent another fragment of PARP. To evidenciate nuclear morphology indicative of apoptosis, another apoptotic hallmark was subsequently assessed by microscopy. In particular, chromatin condensation was demonstrated to occur after 6 h and 12 h treatment of H9c2 cells with ALLN as well as ALLM, as determined by Hoechst 33258 nuclear staining (Fig. 9).

3.6. Apoptosis induced by ALLM is cytochrome c-dependent conversely to ALLN

To our knowledge this is the first report of the effect of ALLN and ALLM on cardiac myoblasts. Therefore, studying the molecular pathways transducing the apoptotic response triggered by ALLN and ALLM appeared intriguing. Thus, the presence of cytochrome c was examined following cytosolic and mitochondrial fractionation. Protein samples of cells treated with either ALLM or ALLN for a time period ranging from 0.5 to 4 h were analyzed by immunoblotting using an anti-cytochrome c antibody. As shown in Fig. 10A top panel, ALLM

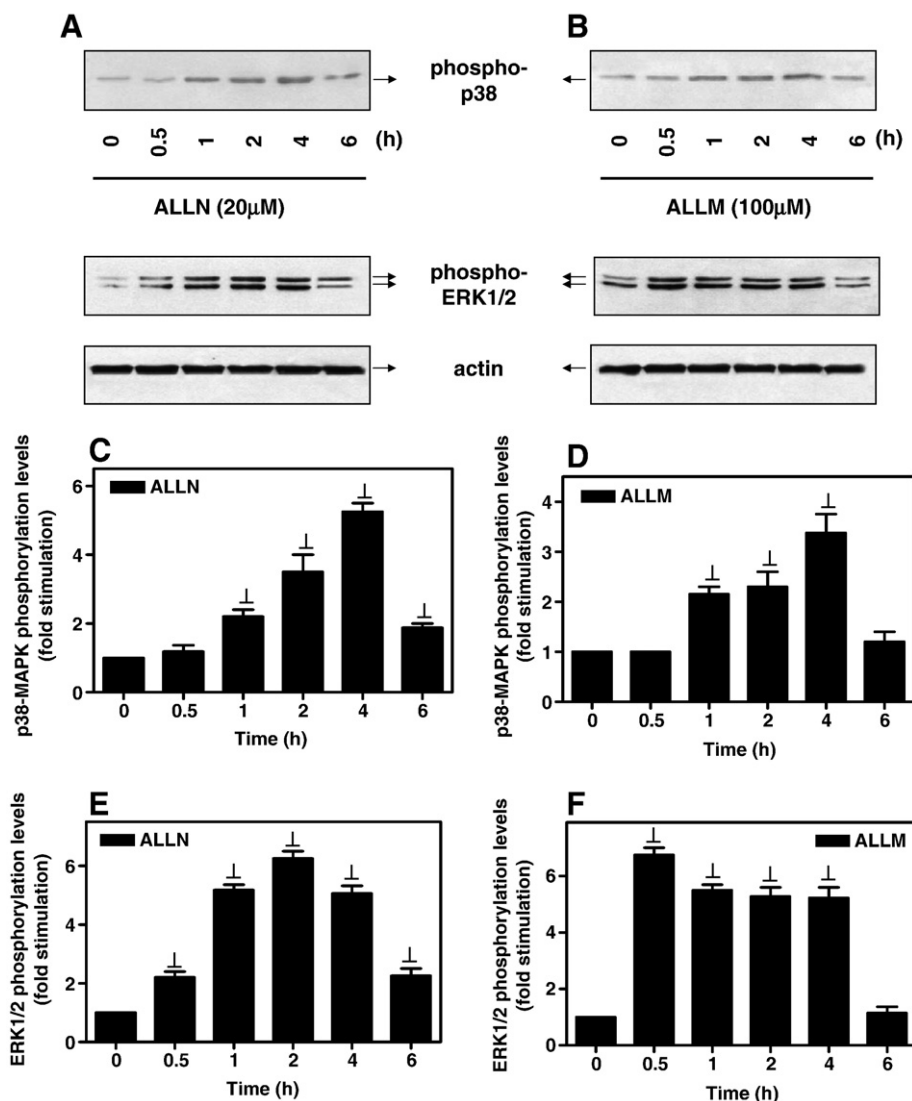


Fig. 6. Time-dependent phosphorylation profile of p38-MAPK and ERKs by ALLN and ALLM in H9c2 cardiomyoblasts. H9c2 cells were exposed to 20 μM ALLN (A) and 100 μM ALLM (B) for the times indicated. Cell extracts (20 μg) were subjected to SDS-PAGE and immunoblotted with antibodies for phosphorylated: p38-MAPK (Thr180/Tyr182) (A and B upper panels), ERKs (Thr202/Tyr204) (A and B middle panels) as well as for total levels of actin (A and B bottom panels). Phospho-p38-MAPK (C and D) and phospho-ERKs (E and F) were quantified by laser scanning densitometry. Blots and results shown are representative of at least three independent experiments. Results are means ± SEM for at least three independent experiments. $p < 0.001$, compared to control values.

induced the rapid release of cytochrome *c* from the mitochondria into the cytosol after 0.5 h treatment (2nd and 7th lines). Equal protein loading was confirmed by reprobing the membrane with an anti-actin antibody (Fig. 10A bottom panel). No translocation of cytochrome *c* was stimulated by ALLN treatment (Fig. 10B) at respective time points. This difference regarding cytochrome *c* participation in the mechanism regulating the observed responses detected, led us to predict that the respective downstream events finally converging at the apoptotic phenotype could also be different. The cleavage of PARP along with the release of cytochrome *c* from the mitochondria observed in ALLM-treated cells, implicated caspase-3 in the pathway activated under these conditions. However, we were unable to detect activation of caspase 3 by these interventions (data not shown). Since phosphorylated αBcr1 has been reported before to interact with pro-caspase 3 limiting its cleavage and therefore hindering caspase 3 activation [37], we made an effort to determine whether phosphorylated αBcr1 could be co-immunoprecipitated with pro-caspase 3 (35 kDa). To this end, anti-caspase 3 was used as the primary antibody in the immunoprecipitation of cell lysates from H9c2 cells left untreated or exposed to ALLN for 2 h and 3 h (Fig. 11A). This antibody recognizes the 35 kDa

pro-caspase 3 as well as the 17 and 19 kDa activated forms of the caspase. The specific anti-phospho-αBcr1 antibody was next used to examine whether pro-caspase 3 could pull down phosphorylated αBcr1. As shown in Fig. 11A, phosphorylation of αBcr1 was detected in the immunoprecipitate of ALLM-exposed cells' lysate, previously incubated with anti-caspase 3 antibody. These findings imply that signalling complexes comprised of phospho-αBcr1 and pro-caspase 3 can be formed under these conditions. The reverse immunoprecipitation was also performed. In particular, caspase 3 immunoreactivity was detected in the immunoprecipitate of ALLM-exposed cells' lysate, previously incubated with anti-phospho-αBcr1 antibody (Fig. 11C). In Fig. 11B the significant reduction of pro-caspase 3 immunoreactivity, after the addition of the respective antibody, is shown. The representative blot in Fig. 11D evidentiates the complete pull-down of phospho-αBcr1 after addition of its specific antibody.

4. Discussion

Heat shock proteins (Hsps) are directly involved in fundamental biological processes, contributing to cell survival under stressful

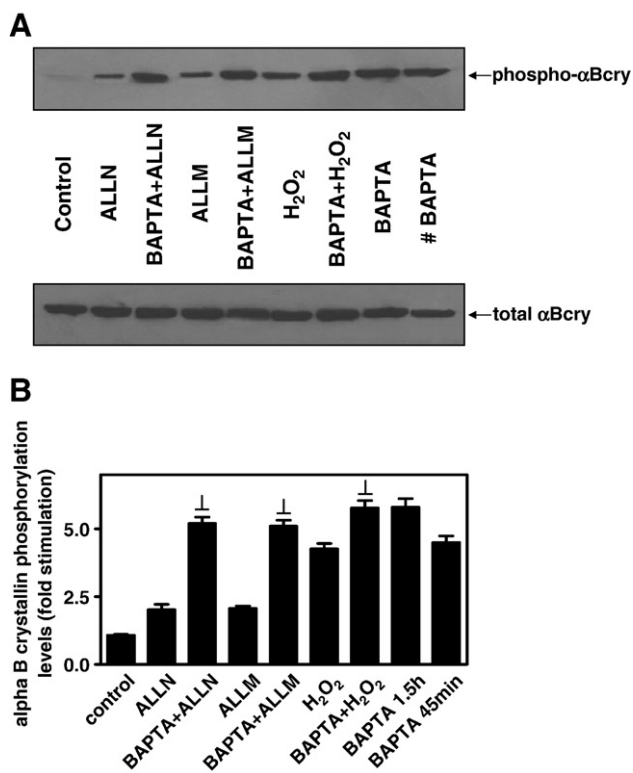


Fig. 7. Effect of BAPTA-AM (10 μ M) on ALLN-, ALLM- and H₂O₂-induced p38-MAPK phosphorylation in H9c2 cardiomyoblasts. H9c2 cells were left untreated (control) or pre-incubated with BAPTA-AM for 30 min and then exposed to 100 μ M ALLM or 20 μ M ALLN for 1 h or to 200 μ M H₂O₂ for 15 min in the absence or presence of BAPTA-AM. Cells incubated with BAPTA-AM alone for either 1.5 h or 45 min (#) were also included. Cell extracts (20 μ g) were subjected to SDS-PAGE and immunoblotted with an antibody for phosphorylated p38-MAPK (A upper panel). To verify equal loading, after stripping, the membranes were incubated with an antibody against total α Bcrystallin (A bottom panel). Bands were quantified by laser scanning densitometry (B). Blots and results shown are representative of at least three independent experiments. Results are means \pm SEM for at least three independent experiments. $p < 0.001$, compared to identically treated cells in the absence of BAPTA-AM.

conditions [38]. In particular, small Hsps (sHsps), have been found to protect cells against various potentially apoptotic stimuli i.e. alpha B-crystallin (α Bcrystallin) preserves lens transparency as well as cardiac function [26] against redox equilibrium disturbances. Quite interestingly, α Bcrystallin presence is considerably abundant in tissues characterized by a high rated oxidative metabolism (e.g. heart, brain, skeletal muscle fibers) [38]. Evidently, it appears important to decipher the signalling mechanisms regulating its response to oxidative stress, a condition known to trigger apoptosis in cardiac myocytes, with the myocardium being exposed to ROS during ischemic insults or various pathological conditions.

Noticeably, we did not detect any stimulation of α Bcrystallin mRNA or total protein levels in H₂O₂-treated H9c2 cells (data not shown). On the contrary, there have been studies reporting upregulation of α Bcrystallin mRNA and protein levels by agents that promote disassembly of microtubules in C6 glioma cells [39] or proteasome inhibition in primary glial cells and oligodendrocytes [40]. The high constitutive expression levels of α Bcrystallin transcripts as well as protein detected in H9c2 cardiac myoblasts may account for this result. What is more, this exceptionally high expression levels in the myocardium may allow α Bcrystallin to exert an immediate protective effect without any lag time necessary for protein synthesis.

An intriguing feature of α Bcrystallin is its post-translational regulation by phosphorylation at three serine sites corresponding to residues 19, 45 and 59 [28]. Corroborating our findings regarding α Bcrystallin exclusive phosphorylation on Ser59, Morrison et al. 2003 [37] have found the

latter to be necessary and sufficient to provide maximal protection of cardiac myocytes from apoptosis induced by hyperosmotic or hypoxic stress. Consistent with the results presented in our study, White et al. 2006 [41] as well as Armstrong et al. 2000 [42] have also observed the single and exclusive phosphorylation of α Bcrystallin at Ser59 following ischemia/reperfusion of rabbit myocardium or ischemic preconditioning of rabbit cardiomyocytes, respectively.

In respect to the pathways mediating this effect, a plethora of studies point to the intermediacy of p38-MAPK in Ser59 phosphorylation [9]. In particular, Hoover et al. 2000 [9] have shown that p38-MAPK pathway cytoprotective effects, in cardiac myocytes exposed to hyperosmotic shock, are due in part to phosphorylation of α Bcrystallin at Ser59. What is more, Shu et al. 2005 [43] have observed p38-MAPK-mediated phosphorylation of α Bcrystallin by PDGF in neonatal mouse ventricular myocytes, with ERKs and JNKs not found to participate in this response. Accordingly, using selective pharmacological inhibitors, we have found p38-MAPK and its downstream substrate MSK1 to be involved in H₂O₂-induced α Bcrystallin (Ser59) phosphorylation (Fig. 1B and D, upper panels). To our knowledge, this is the first report marking MSK1 involvement in α Bcrystallin phosphorylation.

Another original finding of the present study is the detected direct effect of intracellular calcium on α Bcrystallin phosphorylation. Interestingly, Yang et al. 2004 [44] have demonstrated the induction of intracellular [Ca²⁺]_i overload after exposure of cardiomyocytes to H₂O₂ leading to apoptosis. Extracellular calcium levels along with ERKs, JNKs, PKC and PKA were not found to be involved in the observed H₂O₂-induced α Bcrystallin phosphorylation (Fig. 1). On the contrary, investigating the effect of various cytoskeleton stressors, Launay et al. 2006 [3] have shown PKA and PKC to be selectively involved in α Bcrystallin phosphorylation in murine C2C12 myoblasts. Evidently, signalling pathways mediating these respective responses appear to depend on cell type and the nature of the stimulus involved.

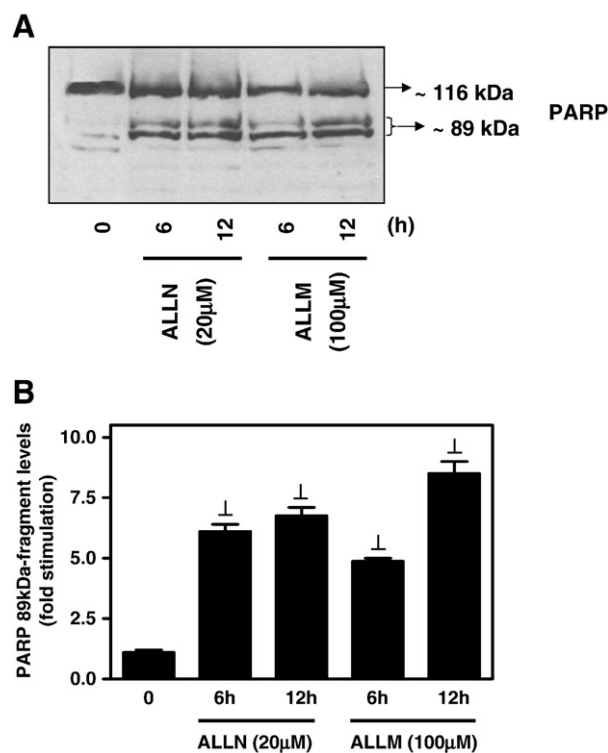


Fig. 8. (A) Profile of PARP cleavage in H9c2 cardiomyoblasts. H9c2 cells were exposed to 20 μ M ALLN and 100 μ M ALLM for the times indicated. (B) Quantification of the 89 kDa PARP fragment by laser scanning densitometry. Blots and results shown are representative of at least three independent experiments. Results are means \pm SEM for at least three independent experiments. $p < 0.001$, compared to control values.

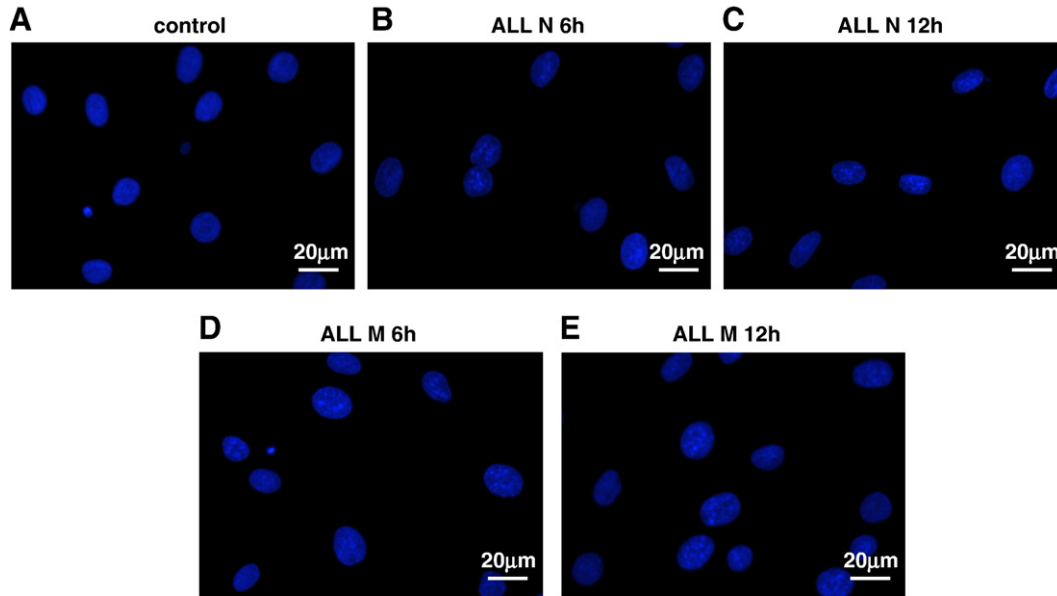


Fig. 9. Nuclear morphology is indicative of apoptosis in ALLN- (20 μ M) (B and C) and ALLM- (100 μ M) (D and E)-treated H9c2 cardiomyoblasts stained with Hoechst 33258. H9c2 cells were left untreated (control) (A) or exposed to 20 μ M ALLN and 100 μ M ALLM for the times indicated. Chromatin condensation was observed in nuclei of cells treated under the aforementioned conditions following staining with Hoechst 33258. Representative images are shown, indicative of at least three independent experiments. (For the colour version of this figure the reader is referred to the web version of this article).

Increased phosphorylation of α Bcr γ contributes to preservation of cytoskeletal architecture [45], mediating cytoprotection by facilitating its interaction with other proteins. Therefore, so as to decipher the role of phosphorylated α Bcr γ in our experimental setting, we next examined its distribution pattern under oxidative stress conditions. The perinuclear and punctuate cytoplasmic localization of phospho- α Bcr γ detected (Fig. 2) combined with its co-localization with tubulin in H_2O_2 -treated H9c2 cells (Fig. 3), is in accordance with multiple studies reporting preservation of microtubular integrity by phosphorylated α Bcr γ , during cardiac ischemia or reperfusion [25,41]. Klemenz et al. 1991 [46] reported the perinuclear localization of α Bcr γ in NIH 3T3 cells exposed to heat shock while Arai and Atomi 1997 [30] demonstrated α Bcr γ chaperone activity to suppress tubulin aggregation in L6 myoblasts. This result is indicative of a potential phospho- α Bcr γ protective role under the interventions investigated in the present study.

We next made an effort to investigate ALLN and ALLM effect on α Bcr γ phosphorylation. ALLN (calpain inhibitor I) as well as ALLM (calpain inhibitor II) are widely used as selective cell-permeable calpain I (micro-calpain) and II (milli-calpain) inhibitors [47]. Calpain was first described as a calcium-dependent cysteine protease by Guroff [48]. Ubiquitously expressed calpains exist in two isoforms μ - and m-calpain activated by micromolar (1–20 μ M) and millimolar (250–750 mM) calcium concentrations, respectively [49]. Evidence suggests their role in turnover of proteins, cytoskeletal organization and cellular death by apoptosis [50]. Nevertheless, their physiological function remains under dispute; several studies have emphasized on calpain inhibition salutary effects i.e. preventing axonal degeneration of opossum optic nerve fibers [33] or reducing infarct size while improving left ventricular contractility in a porcine myocardial ischemia-reperfusion model [51]. However, research groups have also shown calpain repression to induce apoptosis in human acute lymphoblastic leukemia and Non-Hodgkin's lymphoma cells [52] or calpain to be linked to activation of caspase 12 [53] or caspase 7 [54] also leading to apoptosis. Therefore, examining the response stimulated by these two diverse calpain inhibitors appeared to be of primary interest. The concentrations at which ALLN and ALLM have been applied in the present study correlate with the standard doses routinely used in literature [55]. Phosphorylation of α Bcr γ by both ALLN and ALLM was shown to have a similar temporal profile, attaining maximal values at 2 h (Fig. 4) and the prominent role of p38-MAPK and intracellular calcium levels in the observed response was highlighted (Fig. 5), suggesting a linkage of $[Ca^{2+}]_i$ levels, p38-MAPK activation and α Bcr γ phosphorylation in the signalling cascades triggered by both ALLN and ALLM.

MAPK superfamily members have been demonstrated to have a fundamental regulatory role in variable cellular functions i.e. transcription, translation, cell cycle, proliferation, differentiation, senescence and apoptosis [8]. Crosstalk, timing and kinetics of their activation control their ultimate effects. In the present study, p38-MAPK and ERKs were found to be phosphorylated, thus activated, by both ALLN and ALLM (Fig. 6), while no JNKs activation was detected (data not shown). The differential pattern of p38-MAPK and ERKs activation observed might reflect their diverse roles in the particular

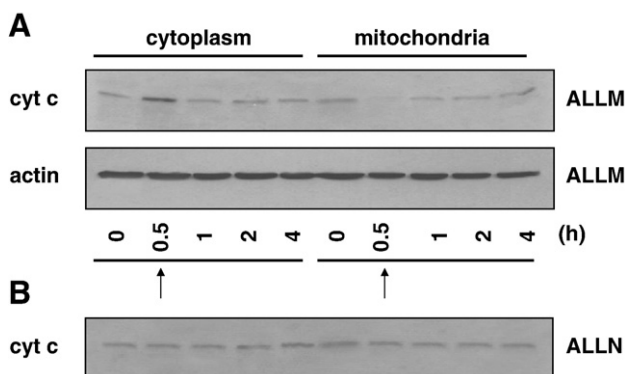


Fig. 10. ALLM-induced translocation of cytochrome c (cyt c) in H9c2 cardiomyoblasts. H9c2 cells were exposed to 100 μ M ALLM (A) and 20 μ M ALLN (B) for the times indicated. Cytoplasmic and mitochondrial cell extracts (20 μ g) were subjected to SDS-PAGE and immunoblotted with an antibody against cytochrome c (A upper panel and B). To verify equal loading, the membranes were then stripped and re-incubated with an antibody against actin (A bottom panel). Blots shown are representative of at least three independent experiments. Arrows indicate the observed translocation of cyt c from mitochondria to the cytoplasm (at 0.5 h of ALLM treatment).

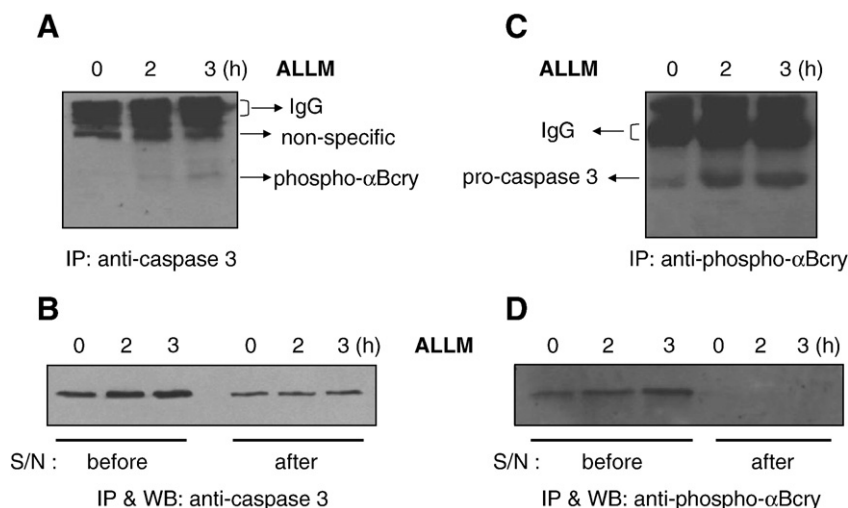


Fig. 11. Co-immunoprecipitation of pro-caspase 3 and phosphorylated α Bcryst in ALLM-treated H9c2 cells. H9c2 cells were exposed to 100 μ M ALLM for the times indicated. Equal amounts of cell lysates were subjected to immunoprecipitation (IP) with the specific antibody against caspase 3 or phosphorylated α Bcryst. The immunoprecipitates were subsequently blotted with the phospho- α Bcryst specific antibody (A) or the antibody against caspase 3 (C). Supernatants (S/N) from untreated or ALLM-treated cells were also blotted for caspase 3 (B) or phosphorylated α Bcryst (D) before and after the addition of the respective antibody, in order to verify their immunodepletion.

experimental setting. One can deduce from Fig. 7 that $[Ca^{2+}]_i$ levels and p38-MAPK activation consist sequential signals mediating the signal transduction mechanism leading to α Bcryst phosphorylation.

Given the discrepancies surrounding calpain inhibition effects on variable cellular functions, we decided to examine the biological impact of H9c2 cells exposure to ALLN and ALLM. To this end, cleavage of PARP [poly-(ADP-ribose) polymerase] was examined. PARPs consist a family of enzymes demonstrating poly-(ADP-ribosyl)ation activity, participating in various biological functions including DNA repair, genomic stability, transcriptional regulation and apoptosis [56]. Cleavage of PARP by caspases 3 or 7 generates fragments of 89 and 24 kDa, a phenomenon widely used as a classical hallmark of apoptosis. Our findings, shown in Fig. 8, revealed the presence of the 89 kDa fragment, indicating involvement of caspases 3 or 7 in the induced apoptotic phenotype after 6 h and 12 h treatment with ALLN or ALLM. Another result substantiating the induction of apoptosis was also the observation of chromatin condensation, determined by Hoechst staining of H9c2 cells nuclei treated under the aforementioned conditions (Fig. 9).

Subsequently, we set out to further probe into the cascade of events leading to apoptosis under these conditions. To this end, cytochrome *c* (cyt *c*) release from mitochondria was examined and found to take place in ALLM-treated cells while ALLN was found to induce apoptosis in a cyt *c*-independent manner (Fig. 10). Therefore, in the case of ALLM, the release of cyt *c* could lead to formation of the apoptosome, recruitment of caspase 9 and activation of downstream effector caspases (i.e. caspase 6 or 7) [57]. On the other hand, ALLN might induce apoptosis through an alternative pathway, possibly bypassing mitochondria, via activation of alternate effectors i.e. caspase 7. Further studies are required in order to specify the step-by-step sequence of biochemical events leading to the observed apoptotic phenotype, given that multiple roles have been attributed to calpain-like proteases in triggering or silencing apoptotic pathways [34]. In particular, one should point out that ALLN has been reported to inhibit cell cycle progression in CHO cells [58] leading to cell death and ALLM has been shown to induce apoptosis in HL-60 cells [34] but also to prevent it in some conditions depending on cell type [31].

A feature that distinguishes these pharmacological agents is also ALLN property to significantly inhibit the proteasome [59]. Within the cell, the proteasome functions as a 26S complex that degrades ubiquitin-conjugated protein molecules contributing to degradation of abnormal or incorrectly synthesized proteins [60] and short-lived

native polypeptides. Therefore, inhibition of the proteasome might lead to accumulation of misfolded, non-functional proteins augmenting further the stress response via perturbation of cellular homeostasis. ALLM has been found to function only as a weak inhibitor of the proteasome and this difference between ALLN and ALLM might also be responsible for the diverse pathways triggered by the latter converging at the apoptotic phenotype.

On the other hand, since proteolysis has been shown to be an essential process in apoptosis and given the prominent role of calpains as proteases, calpain inhibition would be expected to block apoptosis. However, it appears that the signalling pathways involved are complex and that multiple factors regulate eventual cellular fate. Thus, in the presence of MDL28170, another calpain inhibitor, Pineiro et al. 2006 [61] found that calpain-induced proteolysis of caspase 3 was attained in mouse NIH3T3 fibroblasts, leading to activation of the signalling cascade downstream of this caspase. What is more, ALLN was shown to induce caspase 3 activation in insulinoma cells [62]. In our hands, both ALLM and ALLN induced apoptosis via a caspase 3-independent mechanism since no cleaved fragment (17 or 19 kDa) of its precursor molecule was detected under the interventions examined (data not shown). This finding prompted us to look into any probable interaction between α Bcryst and pro-caspase 3 that has been reported before as a characteristic of α Bcryst anti-apoptotic action [63]. Indeed, in the case of ALLM-treated H9c2 cells, the co-immunoprecipitation of phospho- α Bcryst with pro-caspase 3 was demonstrated (Fig. 11). In this context, α Bcryst appears to exert a protective effect partly via blockade of caspase 3 processing. Apoptotic features eventually observed might develop through alternative pathways—overriding caspase 3 inactivation, possibly by other effector caspases and signalling pathways. Thus, depending on the duration of a stressful stimulus, the cell initially responds so as to ensure preservation of viability (i.e. p38-MAPK activation mediating α Bcryst phosphorylation) but if the stress persists, this line of defense is superseded leading to apoptosis.

Overall, our findings provide evidence that oxidative stress as well as calpain inhibition induce phosphorylation of α Bcryst via activation of p38-MAPK and intracellular calcium signalling pathways. The salutary effects of phosphorylated α Bcryst might involve preservation of cytoskeletal integrity or blockade of caspase 3 activation. Evidently, further studies are required to assess the complex nature of these interactions so as to interpret their eventual physiological outcome. Given the strikingly high expression levels of α Bcryst in the cardiac

muscle, that nearly equals the respective amount of major sarcomeric proteins, α Bcr1 is expected to exert a fundamental role in the heart acting as a molecular chaperone that contributes to cell structure and viability preservation. Moreover, considering the detrimental effects of impairments in protein quality control mechanisms, leading to human heart dysfunction, emphasizing on the signalling cascades involved in the regulation of the effectors of this “surveillance process” i.e. the molecular chaperones including α Bcr1, seems compelling.

Acknowledgements

This work was funded by PYTHAGORAS 1 (K.A. 70/3/7399) and by Special Research Account of the University of Athens grants. We would like to thank Dr W. Boelens (Nijmegen, The Netherlands) as well as Dr H. Ito (Aichi, Japan) for kindly providing us with the alpha B-crystallin antibodies used in this study.

References

- [1] M. Vayssier, B.S. Polla, *Cell. Stress Chaperones* 3 (1998) 221–227.
- [2] F. Narberhaus, *Microbiol. Mol. Biol. Rev.* 66 (2002) 64–93.
- [3] N. Launay, B. Goudeau, K. Kato, P. Vicart, A. Lilienbaum, *Exp. Cell Res.* 312 (2006) 3570–3584.
- [4] U. Jakob, M. Gaestel, K. Engels, J. Buchner, *J. Biol. Chem.* 268 (1993) 1517–1520.
- [5] T. Rogalla, M. Ehrnsperger, X. Preville, A. Kotlyarov, G. Lutsch, C. Ducasse, C. Paul, M. Wieske, A.P. Arrigo, J. Buchner, M. Gaestel, *J. Biol. Chem.* 274 (1999) 18947–18956.
- [6] M. Gaestel, *Prog. Mol. Subcell. Biol.* 28 (2002) 151–169.
- [7] J.M. Kyriakis, J. Avruch, *J. Biol. Chem.* 271 (1996) 24313–24316.
- [8] M.A. Bogoyevitch, *Cardiovasc. Res.* 45 (2000) 826–842.
- [9] H.E. Hoover, D.J. Thuerlauf, J.J. Martindale, C.C. Glembotski, *J. Biol. Chem.* 275 (2000) 23825–23833.
- [10] C. Patterson, C. Ike, P.W. Willis, G.A. Stouffer, M.S. Willis, *Circulation* 115 (2007) 1456–1463.
- [11] C. Fumarola, G.G. Guidotti, *Apoptosis* 9 (2004) 77–82.
- [12] D. Acehan, X. Jiang, D.G. Morgan, J.E. Heuser, X. Wang, C.W. Akey, *Mol. Cell* 9 (2002) 423–432.
- [13] A. Glading, D.A. Lauffenburger, A. Wells, *Trends Cell Biol.* 12 (2002) 46–54.
- [14] J.H. Liao, C.C. Hung, J.S. Lee, S.H. Wu, S.H. Chiou, *Biochem. Biophys. Res. Commun.* 244 (1998) 131–137.
- [15] C.S. Alge, S.G. Proglinger, A.S. Neubauer, A. Kampik, M. Zillig, H. Bloemendal, U. Welge-Lüssen, *Invest. Ophthalmol. Vis. Sci.* 43 (2002) 3575–3582.
- [16] G.M. Wang, A. Spector, *Ophthalmol. Vis. Sci.* 36 (1995) 311–321.
- [17] G. Lutsch, R. Vetter, U. Offhaus, M. Wieske, H.J. Grone, R. Klemenz, I. Schimke, J. Stahl, R. Benndorf, *Circulation* 96 (1997) 3466–3476.
- [18] M.J. Kelley, L.L. David, N. Iwasaki, J. Wright, T.R. Shearer, *J. Biol. Chem.* 268 (1993) 18844–18849.
- [19] L.L. David, J.W. Wright, T.R. Shearer, *Biochim. Biophys. Acta* 1139 (1992) 210–216.
- [20] M.R. Duchon, *J. Physiol. (London)* 529 (2000) 57–68.
- [21] B.W. Kimes, B.L. Brandt, *Exp. Cell Res.* 98 (1976) 367–381.
- [22] N. Turner, F. Xia, G. Azhar, X. Zhang, L. Liu, J. Wei, *J. Mol. Cell. Cardiol.* 30 (1998) 1789–1801.
- [23] I.K. Aggeli, C. Gaitanaki, I. Beis, *Cell. Signal.* 18 (2006) 1801–1812.
- [24] R.A. Gottlieb, D.J. Granville, *Methods* 26 (2002) 341–347.
- [25] W.F. Bluhm, J.L. Martin, R. Mestrlil, W.H. Dillmann, *Am. J. Physiol.* 275 (1998) H2243–H2249.
- [26] J.L. Martin, R. Mestrlil, R. Hilal-Dandan, L.L. Brunton, W.H. Dillmann, *Circulation* 96 (1997) 4343–4348.
- [27] K. Ishikawa, S. Kimura, A. Kobayashi, T. Sato, H. Matsumoto, Y. Ujje, K. Nakazato, M. Mitsugi, Y. Maruyama, *Circ. J.* 69 (2005) 617–620.
- [28] H. Ito, K. Okamoto, H. Nakayama, T. Isobe, K. Kato, *J. Biol. Chem.* 272 (1997) 29934–29941.
- [29] S.A. Cook, P.H. Sugden, A. Clerk, *Circ. Res.* 85 (1999) 940–949.
- [30] H. Arai, Y. Atomi, *Cell. Str. Fun.* 22 (1997) 539–544.
- [31] M.K.T. Squier, A.C.K. Miller, A.M. Malkinson, J.J. Cohen, *J. Cell. Physiol.* 159 (1994) 229–237.
- [32] L.A. Casciola-Rosen, D.K. Millers, G.J. Anhalt, A. Rosen, *J. Biol. Chem.* 269 (1994) 30757–30760.
- [33] L.A. Couto, M.S. Narciso, J.N. Hokoc, A.M. Blanco-Martinez, *J. Neurosci. Res.* 77 (2004) 410–419.
- [34] Q. Lu, R.L. Mellgren, *Arch. Biochem. Biophys.* 334 (1996) 175–181.
- [35] A. Strasser, L. O'Connor, V.M. Dixit, *Annu. Rev. Biochem.* 69 (2000) 217–245.
- [36] D.W. Nicholson, *Cell Death Differ.* 6 (1999) 1028–1042.
- [37] L.E. Morrison, H.E. Hoover, D.J. Thuerlauf, C.C. Glembotski, *Circ. Res.* 92 (2003) 203–211.
- [38] A.P. Arrigo, S. Simon, B. Gibert, C. Kretz-Remy, M. Nivon, A. Czekalla, D. Guillet, M. Moulin, C. Diaz-Latoud, P. Vicart, *FEBS Lett.* 581 (2007) 3665–3674.
- [39] K. Kato, H. Ito, Y. Inaguma, K. Okamoto, S. Saga, *J. Biol. Chem.* 271 (1996) 26989–26994.
- [40] O. Goldbaum, C. Richter-Landsberg, *J. Neurosci.* 24 (2004) 5748–5757.
- [41] M.Y. White, B.D. Hambly, R.W. Jeremy, S.J. Cordwell, *J. Mol. Cell. Cardiol.* 40 (2006) 761–774.
- [42] S.C. Armstrong, C.L. Shivell, C.E. Ganote, *J. Mol. Cell. Cardiol.* 32 (2000) 1301–1314.
- [43] E. Shu, H. Matsuno, S. Akamastu, Y. Kanno, H. Suga, K. Nakajima, A. Ishisaki, S. Takai, K. Kato, Y. Kitajima, O. Kozowa, *Arch. Biochem. Biophys.* 438 (2005) 111–118.
- [44] K.T. Yang, S.F. Pan, C.L. Chien, S.M. Hsu, Y.Z. Tseng, S.M. Wang, M.L. Wu, *FASEB J.* 18 (2004) 1442–1444.
- [45] P.J. Muchowski, G.J. Wu, J.J. Liang, E.T. Adman, J.I. Clark, *J. Mol. Biol.* 289 (1999) 397–411.
- [46] R. Klemenz, E. Frohli, R.H. Steiger, R. Schafer, A. Aoyama, *Proc. Natl. Acad. Sci. U. S. A.* 88 (1991) 3652–3656.
- [47] L. Zhang, L. Song, E.M. Parker, *J. Biol. Chem.* 274 (1999) 8966–8972.
- [48] G. Guroff, *J. Biol. Chem.* 239 (1963) 149–155.
- [49] K. Suzuki, S. Imajoh, Y. Emori, H. Hawashima, Y. Minami, S. Ohno, *FEBS Lett.* 220 (1987) 271–277.
- [50] G.Y. Huh, S.B. Glantz, J.S. Morrow, J.H. Kim, *Neurosci. Lett.* 316 (2001) 41–44.
- [51] P.N. Khalil, C. Neuhof, R. Huss, M. Pollhammer, M.N. Khalil, H. Neuhof, H. Fritz, M. Siebek, *Eur. J. Pharmacol.* 528 (2005) 124–131.
- [52] D.M. Zhu, F.M. Uckun, *Clin. Cancer Res.* 6 (2000) 2456–2463.
- [53] R.W. Neumar, Y.A. Xu, H. Gulaf, R.P. Guttmann, R. Siman, *J. Biol. Chem.* 278 (2003) 14162–14167.
- [54] B.B. Wolf, M. Schuler, E. Kaheveti, D.R. Green, *J. Biol. Chem.* 274 (1999) 30651–30656.
- [55] Y. Ihara, Y. Urata, S. Goto, T. Kondo, *Am. J. Physiol.* 290 (2006) C208–C221.
- [56] A. Burkle, *FEBS J.* 272 (2005) 4576–4589.
- [57] P. Li, D. Nijhawan, I. Budihardjo, S.M. Srinivasule, M. Ahmad, E.S. Alnemri, X. Wang, *Cell* 91 (1997) 479–489.
- [58] S.W. Sherwood, A.L. Kung, J. Roitelman, R.D. Simoni, R.T. Schimke, *Proc. Natl. Acad. Sci. U. S. A.* 90 (1993) 3353–3357.
- [59] K.L. Rock, C. Gramm, L. Rothstein, K. Clark, R. Stein, L. Dick, D. Hwang, A.L. Goldberg, *Cell* 78 (1994) 761–771.
- [60] C.L. Ward, S. Omura, R.R. Kopito, *Cell* 83 (1995) 121–127.
- [61] D. Pineiro, M.E. Martin, N. Guerra, M. Salinas, V.M. Gonzalez, *Exp. Cell Res.* 313 (2007) 369–379.
- [62] J. Storling, N. Allaman-Pillet, A.E. Karlsen, N. Billestrup, C. Bonny, T. Mandrup-Poulsen, *Endocrinology* 146 (2005) 1718–1726.
- [63] Y.W. Mao, J.P. Liu, H. Xiang, D.W.C. Li, *Cell Death Differ.* 11 (2004) 512–526.